The Average Mass Profile of Galaxy Clusters

R. G. Carlberg[1,2], H. K. C. Yee[1,2], E. Ellingson[1,3], S. L. Morris[1,4], R. Abraham[1,4,5], P. Gravel[1,2], C. J. Pritchet[1,6], T. Smecker-Hane[1,4,7] F. D. A. Hartwick[6] J. E. Hesser[4], J. B. Hutchings[4], & J. B. Oke[4]

ABSTRACT

The average mass density profile measured in the CNOC cluster survey is well described with the analytic form $\rho(r) = A r^{-1}(r + a_\rho)^{-2}$, as advocated on the basis on n-body simulations by Navarro, Frenk & White. The predicted core radii are $a_\rho = 0.20$ (in units of the radius where the mean interior density is 200 times the critical density) for an $\Omega = 0.2$ open CDM model, or $a_\rho = 0.26$ for a flat $\Omega = 0.2$ model, with little dependence on other cosmological parameters for simulations normalized to the observed cluster abundance. The dynamically derived local mass-to-light ratio, which has little radial variation, converts the observed light profile to a mass profile. We find that the scale radius of the mass distribution, $0.20 \leq a_\rho \leq 0.30$ (depending on modeling details, with a 95% confidence range of $0.12 - 0.50$), is completely consistent with the predicted values. Moreover, the profiles and total masses of the clusters as individuals can be acceptably predicted from the cluster RMS line-of-sight velocity dispersion alone. This is strong support of the hierarchical clustering theory for the formation of galaxy clusters in a cool, collisionless, dark matter dominated universe.

Subject headings: galaxies: clusters, cosmology: large-scale structure of universe

---

[1]Visiting Astronomer, Canada–France–Hawaii Telescope, which is operated by the National Research Council of Canada, le Centre National de Recherche Scientifique, and the University of Hawaii.

[2]Department of Astronomy, University of Toronto, Toronto ON, M5S 3H8 Canada

[3]Center for Astrophysics & Space Astronomy, University of Colorado, CO 80309, USA

[4]National Research Council of Canada, Herzberg Institute of Astrophysics, Dominion Astrophysical Observatory, 5071 West Saanich Road, Victoria, BC, V8X 4M6, Canada

[5]Institute of Astronomy, Madingley Road, Cambridge CB3 0HA, UK

[6]Department of Physics & Astronomy, University of Victoria, Victoria, BC, V8W 3P6, Canada

[7]Department of Physics & Astronomy, University of California, Irvine, CA 92717, USA

1. Introduction

A fundamental prediction of the hierarchical clustering paradigm in a collisionless dark matter dominated universe is that the average mass profile of dark halos must primarily depend on mass, if the density perturbation spectrum is nearly a power law. The single parameter surface brightness profile, $\Sigma \propto \exp\left(-r^{1/4}\right)$, was proposed by deVaucouleurs (1948) to describe elliptical galaxies, but it was later found also to be quite an accurate description of isolated n-body collapse simulations, both with and without dissipation (van Albada 1982, Carlberg, Lake & Norman 1986). This $r^{1/4}$ "law" has no simple analytic form to describe the volume distribution (Young 1976), motivating Hernquist (1990) to propose the function $\rho_H(r) = Ar^{-1}(r + a)^{-3}$ as a more tractable alternative, which in projection is usefully close to the $r^{1/4}$ function.

In cosmological halo formation simulations, where external tides and continuing infall are included, the central density profile is found to remain approximately r^{-1} (Dubinski & Carlberg 1991, Carlberg 1994, Syer & White 1996), although there is growing evidence that the central slope is somewhat steeper (Fukushige & Makino 1997, Evans & Collett 1997). However, beginning near the virialization radius the density profile is found to fall somewhat less steeply than in isolated collapses, leading Navarro, Frenk & White (1996 and 1997, hereafter NFW) to advocate $\rho(r) = Ar^{-1}(r + a)^{-2}$ as an empirical description of the halo density profiles. In a series of exhaustive n-body simulations the relation between the scale radius, a, of the halo and its mass has been studied to yield an empirical understanding of its value (Cole & Lacey 1996, NFW). The principal result of interest here is that the scale radius, a, is measured in the simulations to be about 20% of the "virial radius" for the $10^{15}\,M_\odot$ dark halos appropriate to rich clusters. This result has only a weak dependence on either the power spectrum, or the world model parameters Ω and Λ, for simulations normalized to the observed cluster abundance. Halos of much lower mass, say the $10^{12}\,M_\odot$ characteristic of individual galaxies, are generally much more centrally concentrated than clusters, with quite a strong dependence on the cosmological details.

In the next section we fit the galaxy number density profile, $\nu(r)$, to the NFW function, then present evidence that this profile (specifically for galaxies selected in Gunn r, which as a red pass band is relatively insensitive to the current star formation rate) accurately traces the average cluster mass profile, $\rho(r)$. In particular we compare the derived surface mass profile with the surface galaxy number profile. Our analysis is independent of the light-traces-mass assumption and allows for a range of velocity dispersion profiles. We have previously shown that this type of analysis works to recover the same mass profile from two vastly different subsamples of the data (Carlberg *et al.* 1997a). The fitted scale radius of the NFW model is compared to the predicted scale radius. In Section 3, we use the scaling from velocity dispersion to radius to predict the form of the profile for each cluster in turn and compare it to the available data. The results are briefly discussed in the final section. We use $H_0 = 100\,\mathrm{km\,s^{-1}\,Mpc^{-1}}$ and $\Omega_0 = 2q_0 = 0.2$ for all our calculations, although the results are not very sensitive to these choices.

2. The Average Mass Profile of a Galaxy Cluster

The Canadian Network for Observational Cosmology (CNOC) Cluster Survey (Carlberg *et al.* 1994, Yee, Ellingson & Carlberg 1996) obtained ~ 2600 redshifts of Gunn r selected galaxies in the fields of 16 high luminosity X-ray clusters at $z \sim 1/3$. This is a relatively homogeneous sample of clusters that are guaranteed to be at least partially virialized on the basis of their X-ray emission. The virial mass-to-light ratios of these clusters were found to be identical, within their measurement errors of $\sim 25\%$ (Carlberg *et al.* 1996). The 14 clusters that are "non-binary" are combined in normalized co-ordinates to make an ensemble cluster. This diminishes substructure and asphericity to a level where the galaxies can be treated as if in a spherical distribution which is consistent with dynamical equilibrium (Carlberg *et al.* 1997a). Galaxies of all colors above a k-corrected Gunn r absolute magnitude of -18.5 are included in the average.

2.1. The Average Cluster Number Density Profile

To combine the clusters the brightest cluster galaxy (BCG) is used as the nominal center of each cluster on the sky following our earlier procedures (Carlberg, Yee & Ellingson 1997, hereafter CYE). The galaxy velocities are normalized to σ_1, the RMS velocity dispersion of the clusters about the cluster mean. The projected radii are normalized to an empirically determined r_{200}, the radius where the mean interior overdensity is $200\rho_c$. To derive r_{200} from the observational virial radius, r_v (which is largely fixed by the outer boundary of the sample), we assume that $M(r) \propto r$. This gives

$$r_{200} = \frac{\sqrt{3}}{10} \frac{\sigma_1}{H(z)}, \tag{1}$$

which is completely independent of the observational virial radius. Usually the extrapolation in radius is a modest 25%, so the precise mass profile assumed makes little difference to the result (CYE).

The average projected galaxy number density profile, $\Sigma(R)$, is fit with the projection of the volume density function,

$$\nu(r) = \frac{A}{r(r + a_\nu)^p}, \tag{2}$$

where p is fixed at either $p = 2$ (NFW) or $p = 3$ (Hernquist). The results for $p = 2$ are shown in Figure 1 as the solid line. The dashed lines are described below. Both the $p = 2$ and $p = 3$ forms are statistically acceptable fits by the χ^2 test. We will only consider the $p = 2$ form for the rest of this paper. The fitted scale radius is $a_\nu = 0.27$ with a 95% confidence range of $0.13 - 0.43$ from the χ^2 distribution.

2.2. The Relationship between the Mass and Number Density Profiles

There is no dynamical necessity for $\nu(r)$ to be directly proportional to $\rho(r)$. The relationship between the two is derived from the projected velocity dispersion, $\sigma_p(R)$. The dynamical mass profile, $M_D(r)$, which is the volume integral of $\rho(r)$, is inferred from the Jeans Equation (*e.g.* , Binney & Tremaine 1987, CYE),

$$M_D(r) = -\frac{\sigma_r^2 r}{G}\left[\frac{d\ln\sigma_r^2}{d\ln r} + \frac{d\ln\nu}{d\ln r} + 2\beta\right], \tag{3}$$

where the velocity anisotropy parameter, $\beta = 1 - \sigma_\theta^2/\sigma_r^2$. N-body simulations for a variety of cosmologies show that the dependence of β has a nearly universal radial variation (Cole & Lacey 1996) which we somewhat arbitrarily model as,

$$\beta(r) = \beta_m\frac{4r}{r^2+4}, \tag{4}$$

which takes on a maximum value of β_m at $r = 2$, in r_{200} units. We demonstrate below that the volume *mass* density is not very sensitive to the details of the velocity modeling, provided the model is an acceptable statistical description of the data. We use values of 0.3 and 0.5 for the parameter β_m which roughly bracket the range of β seen in the simulations.

We model the radial velocity dispersion as,

$$\sigma_r^2 = B\frac{c_1 r/(1+c_1 r) + c_2}{1 + r/b}, \tag{5}$$

where B and b are the two parameters adjusted to fit the observed $\sigma_p(R)$. We include here a new central data point at $0.05r_{200}$. The rest of the data are as in CYE. The $[c_1, c_2]$ parameters are externally fixed to allow us to vary the shape of the curve. In Figure 2 we display results where $[c_1, c_2]$ are $[0, 1]$ and $[1, 0]$ to give the two extremes of the functional form. The $[0, 1]$ form was used in CYE and $[1, 0]$ gives a dispersion which drops to zero at the center. The intermediate values $[8, 1/2]$ are adopted for reasons made clear below. Both the $[1, 0]$ and $[8, 1/2]$ forms have reduced χ^2 near unity. The $[0, 1]$ form is about 4% probable, although this is critically dependent on the $0.05r_{200}$ point, the concern being that the old central galaxies may be a distinct, low velocity dispersion, cluster population.

We show the results of the mass analysis in Figure 3. The quantity plotted is $\rho(r)/\nu(r)$ normalized to $M_v/L \times L(r)$, computed from the same data. The ratio $\rho(r)/\nu(r)$ is only weakly constrained inside $0.1r_{200}$ and the assumption of virialization likely fails outside $1.5r_{200}$. Within this radial range $\rho(r)/\nu(r)$ varies less than about 30% of its mean value. It should be noted that for most purposes the more relevant quantity is $M_D(r)$, the volume integral of $\rho(r)$, which is substantially more slowly varying. The offset of $\rho(r)/\nu(r)$ below unity indicates that mass and light are similarly distributed but that the virial mass has a scale error. A wide range of positive intermediate values of c_1 and c_2 gives nearly constant b_{Mv} everywhere. We display the $c_1 = 8$,

$c_2 = 1/2$ case, which is one of many intermediate sets of parameters which leads to substantial cancellation of the opposite behaviour of the two extreme $\sigma_r(r)$ models in the derived $M_D(r)$.

With the dynamically derived $\rho(r)/\nu(r)$ in hand we can use it to model the galaxy number profile, $\nu(r)$, assuming the *mass* profile is described by the NFW profile. This procedure measures a_ρ, the scale radius of the *mass* distribution. We take $\rho(r)/\nu(r)$ to be equal to the endpoint of the range for $r < 0.1r_{200}$ and $r > 1.5r_{200}$. The results for our three velocity dispersion functions and the two values of β_m are shown in Figure 1 as the dashed lines. The resulting a_ρ values range from 0.20 ($[c_1, c_2] = [0, 1]$) to 0.30 ($[1, 0]$). This expands the 95% confidence range of a_ρ over a_ν slightly, to $0.12 \leq a_\rho \leq 0.50$. We conclude that galaxies selected from their red light brightness, *i.e.* , a passband well to the red of the 4000Å break to minimize sensitivity to star formation (and not necessarily galaxies red in color, Carlberg *et al.* 1997a), accurately trace the mass profile of the cluster. That is, $\nu(r)$ is directly proportional to $\rho(r)$, within the statistical limits of our measurements.

3. Individual Cluster Profiles

The NFW profile can be tested for its application to the clusters as individuals. The r_{200} for each cluster is derived from the observed velocity dispersion, Equation 1. The NFW scale radius is set at our best fit value, $a_\nu = 0.27$. The fits are restricted to the region inside $1.5r_{200}$, which is expected to be virialized for $\Omega \simeq 0.2$. The resulting χ^2 per degree of freedom (there being 10-16 degrees of freedom) are given in Table 1. The cluster MS0906+11, which we observed, is excluded because it was not possible to measure a reliable velocity dispersion, which we believe is likely because there is another nearby clusters in the redshift direction (Carlberg *et al.* 1996). The reduced χ^2 values of 14 of the 15 clusters are 1.1 or less, indicating that the NFW function with a fixed scale radius is a statistically acceptable fit to the density profile. The A2390 cluster has $\chi^2 = 1.38$ per degree of freedom which indicates that the fit is about 15% probable. A2390 is the cluster with the most data. If we had about a third less data for this cluster, the fit would have been entirely acceptable. However, as the amount of cluster data increases beyond about 100 galaxies, the substructure within the cluster (Abraham *et al.* 1996) becomes more clearly detected. By extension, if we had obtained more than 200 or so galaxies within any cluster, the substructure would have become clearly resolved. This sampling strategy was part of the initial layout of the CNOC observations.

4. Discussion and Conclusions

We have established that the dynamical mass profile, $\rho(r)$, is proportional to the galaxy number density profile, $\nu(r)$, over the range of radii where the argument is secure. We further make the modest assumption that $\nu(r)$ continues to trace the mass, within the errors, at larger

radii. Consequently we conclude that the NFW function accurately describes the mass field. The measured scale radius is $0.20 \leq a_\rho \leq 0.30$ with a 95% confidence range of $0.12 - 0.50$. This relatively large confidence range is a result of the relatively small change in profile slope at the characteristic scale for the NFW profile. The Hernquist function has much smaller errors when used in same fitting procedure. The predicted values for $\Omega = 0.2$ and a CDM spectral normalization of $\sigma_8 = 0.95$ are 0.20 for an open model (nearly identical to the $\sigma_8 = 0.6$, $\Omega = 1$ value of 0.19) and 0.26 for a flat low density model (NFW), are remarkably precise predictions of the observed value.

Overall it appears that a very good understanding of the evolution of the mass field in clusters is emerging. The value of Ω determined from dynamical observations of clusters (Carlberg *et al.* 1996, CYE) predicts a slow change in the abundance of clusters with redshift, which is in accord with the directly observed value (Carlberg *et al.* 1997b). Previously we found that clusters as individuals have masses inside r_{200} which are accurately predicted from their velocity dispersions (Carlberg *et al.* 1996). Here we have shown that the predicted scale radius and the universal NFW profile provide a statistically acceptable description of the virialized region, $r \leq 1.5r_{200}$, of 14 of the 16 clusters selected for the CNOC observational program, with the failures likely being the result of large substructures. The combination of successful predictions of galaxy cluster mass profiles and their cosmological number density evolution is a strong argument for the model of cluster formation in an effectively cold, collisionless, dark matter dominated universe. These results could be substantially tightened, in the first instance, through redshift determinations for more cluster galaxies in the outskirts of this sample.

REFERENCES

Abraham, R. G., Smecker-Hane, T. A., Hutchings, J. B., Carlberg, R. G., Yee, H. K. C., Ellingson, E., Morris, S. L., Oke, J. B., Davidge, T. 1996, ApJ, 471, 694

Binney, J. & Tremaine, S. 1987, *Galactic Dynamics*, (Princeton University Press)

Carlberg, R. G., Lake, G. L., and Norman, C. A. 1986, ApJ, 300, L1

Carlberg, R. G. 1994, ApJ, 433, 468

Carlberg, R. G., Yee, H. K. C., Ellingson, E., Pritchet C., Abraham, R., Smecker-Hane, T., Bond, J. R., Couchman, H. M. P., Crabtree, D., Crampton, D., Davidge, T., Durand, D., Eales, S., Hartwick, F. D. A., Hesser, J. E., Hutchings, J. B., Kaiser, N., Mendes de Oliveira, C., Myers, S. T., Oke, J. B., Rigler, M. A., Schade, D., & West, M. 1994, JRASC, 88, 39

Carlberg, R. G., Yee, H. K. C., Ellingson, E., Abraham, R., Gravel, P., Morris, S. L., & Pritchet, C. J. 1996, ApJ, 462, 32

Carlberg, R. G., Yee, H. K. C., & Ellingson, E. 1997, ApJ, in press (CYE)

Carlberg, R. G., Yee, H. K. C., Ellingson, E., Morris, S. L., Abraham, R., Gravel, P., Pritchet, C. J., Smecker-Hane, T., Hartwick, F. D. A., Hesser, J. E., Hutchings, J. B., & Oke, J. B. 1997a, ApJ, 476, L7

Carlberg, R. G., Morris, S. L., Yee, H. K. C., & Ellingson, E. 1997b, ApJ, 479, L19

Cole, S. & Lacey, C. G. 1996, MNRAS, 281, 716

de Vaucouleurs, G. 1948, *Ann. d'Ap.* 11, 247

Dubinski, J. & Carlberg, R. G. 1991, ApJ, 378, 496

Evans, N. W. & Collett, J. L. 1997, MNRAS, submitted (astroph/9702085)

Fukushige, T. & Makino, J. 1997, ApJ, in press (astroph/9610005)

Hernquist, L. 1990, ApJ, 356, 359

Navarro, J. F., Frenk, C. S. & White, S. D. M. 1996, ApJ, 462, 563

Navarro, J. F., Frenk, C. S. & White, S. D. M. 1997, ApJ, submitted (astro-ph/9611107, NFW)

Syer, D. & White, S. D. M. 1996, MNRAS, submitted (astroph/9611065)

van Albada, T. S. 1982, MNRAS, 201, 939

Yee, H. K. C., Ellingson, E. & Carlberg, R. G. 1996, ApJS, 102, 269

Young, P. J. 1976, AJ, 81, 907

Table 1: Goodness of Fit of A Universal Profile

Name	χ^2/ν	# cluster redshifts
A2390	1.38	178
MS0016+16	0.49	47
MS0302+16	0.88	26
MS0440+02	0.62	37
MS0451+02	0.76	114
MS0451−03	0.83	50
MS0839+29	0.98	45
MS1006+12	0.50	28
MS1008−12	0.70	67
MS1224+20	1.10	24
MS1231+15	0.69	76
MS1358+62	0.57	171
MS1455+22	0.69	55
MS1512+36	0.48	38
MS1621+26	0.88	96

Fig. 1.— The average galaxy density profile of the clusters using the BCG as the center. In the text, we demonstrate that this galaxy number density profile is statistically equal to the projected average mass profile. The solid line is the projection of the NFW function. The dotted lines are the projection of the product of an assumed NFW *mass* profile with the dynamically derived local light-to-mass ratio, $\nu(r)/\rho(r)$. The dashed lines are the projected NFW mass profiles themselves, offset downward by half a dex.

Fig. 2.— The projected velocity dispersion profile and the projection of the fitted profiles, for both $\beta_m = 0.3$ and 0.5 which are nearly indistinguishable on this plot. The dotted line is for $[c_1, c_2] = [0, 1]$, the dashed for $[1, 0]$ and the solid is $[8, 1/2]$ (see text for details).

Fig. 3.— The derived ratio of the dynamical mass density profile, $\rho(r)$, to r selected galaxy profile, $\nu(r)$, normalized with the virial mass-to-light ratio evaluated inside $1.5r_{200}$. In each pair of curves the upper line at small radius is for $\beta_m = 0.3$ and the lower for $\beta_m = 0.5$. The dotted line is for $c_1 = 0$, the dashed for $c_2 = 0$ and the solid is our preferred $c_1 = 8$, $c_2 = 1/2$.
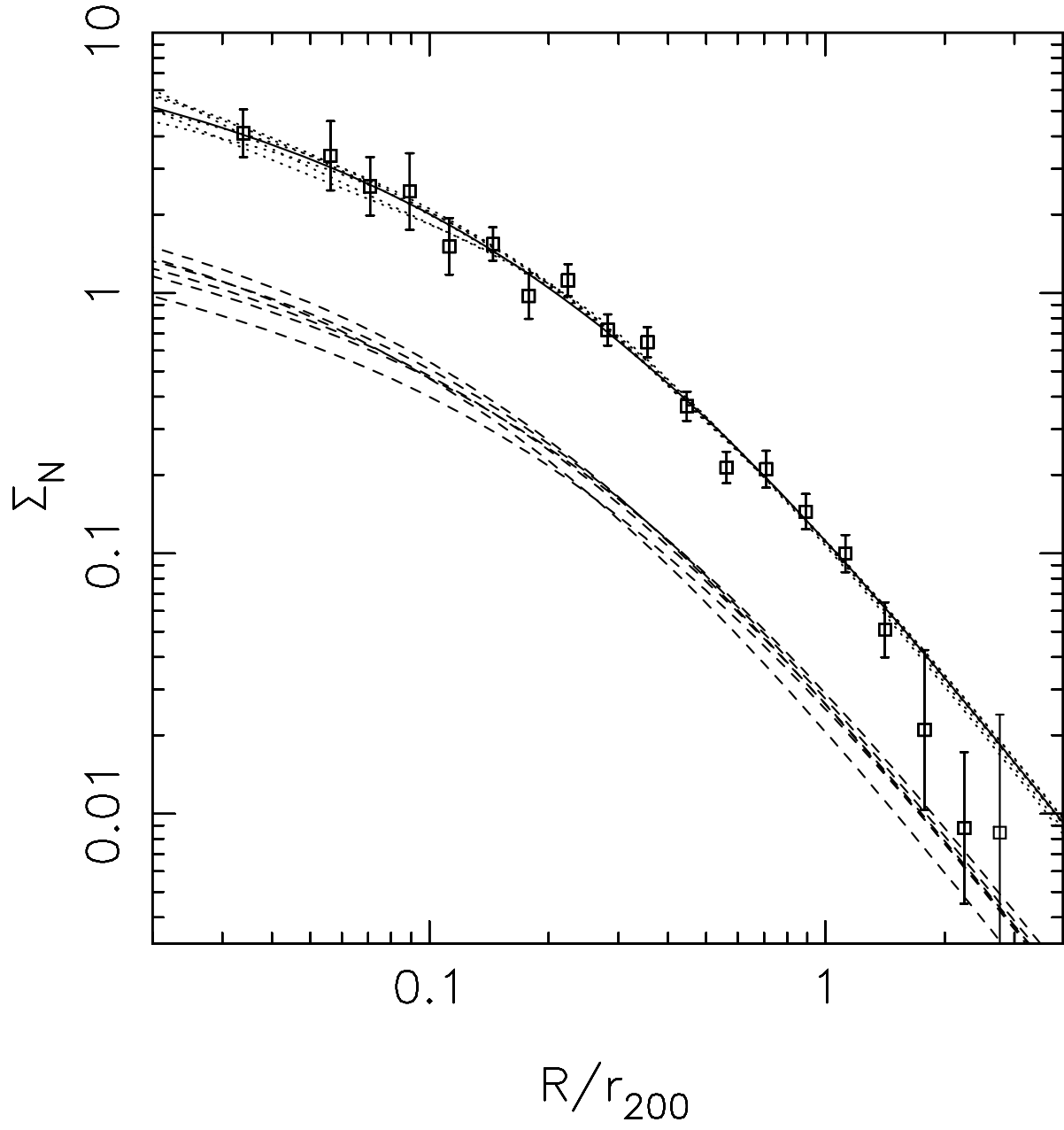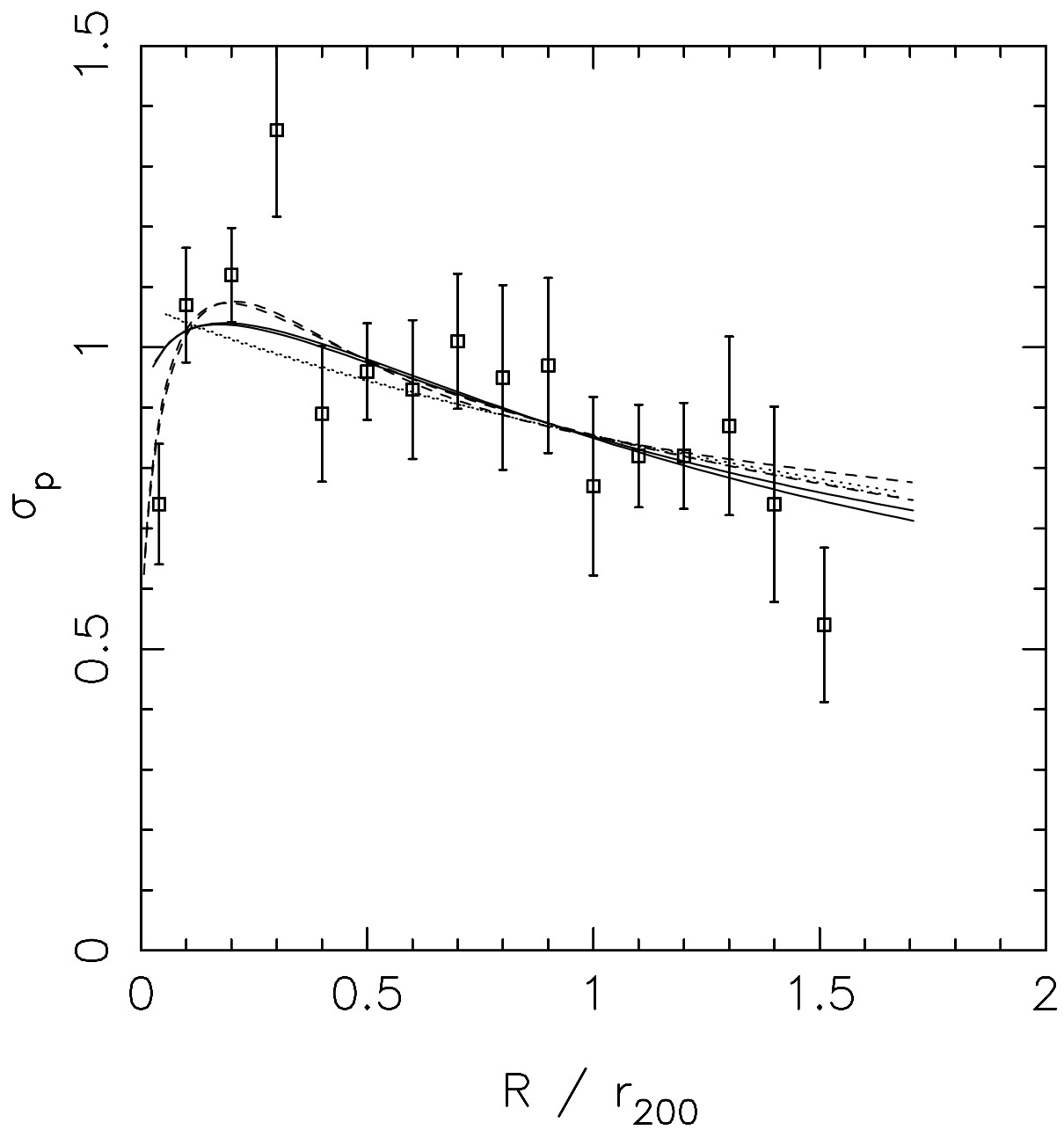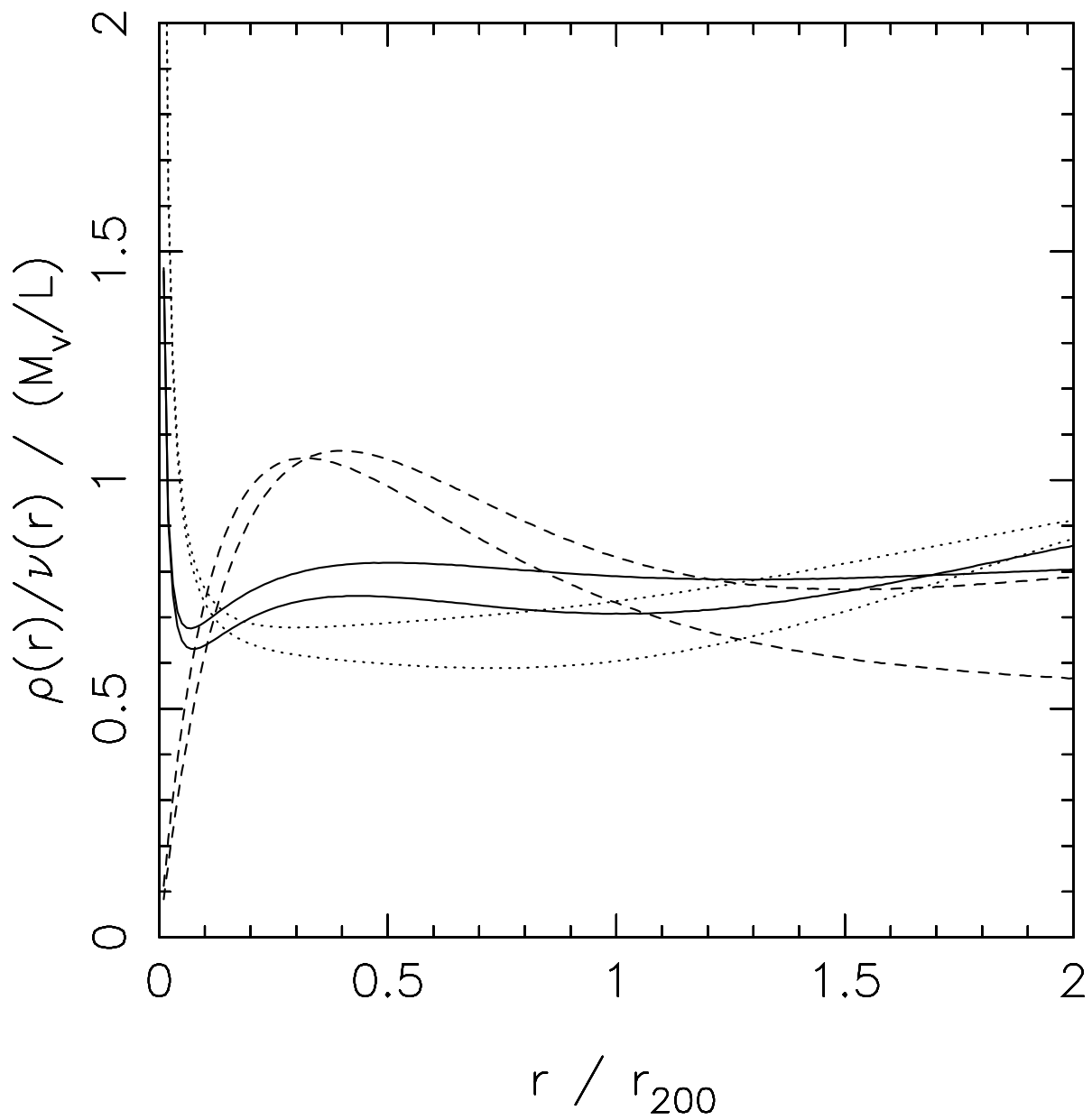
Fig. 1.—

Fig. 2.—

Fig. 3.—